JACS
JOURNAL OF THE AMERICAN CHEMICAL SOCIETY
Cite This: J. Am. Chem. Soc. 2018, 140, 7799−7802
Communication
pubs.acs.org/JACS

Ter-Ionic Complex that Forms a Bond Upon Visible Light Absorption

Sara A. M. Wehlin,[§,†] Ludovic Troian-Gautier,[§,†] Renato N. Sampaio,[†] Lionel Marcélis,[‡] and Gerald J. Meyer*[,†]

[†]Department of Chemistry, University of North Carolina at Chapel Hill, Murray Hall 2202B, Chapel Hill, North Carolina 27599-3290, United States

[‡]Engineering of Molecular NanoSystems, Ecole Polytechnique de Bruxelles, Université libre de Bruxelles (ULB), Avenue F.D. Roosevelt 50, CP165/64, B-1050 Brussels, Belgium

Supporting Information

ABSTRACT: A "ter-ionic complex" composed of a tetracationic Ru(II) complex and two iodide ions was found to yield a covalent I−I bond upon visible light excitation in acetone solution. ^{1}H NMR, visible absorption and DFT studies revealed that one iodide was associated with a ligand while the other was closer to the Ru metal center. Standard Stern−Volmer quenching of the excited state by iodide revealed upward curvature with a novel saturation at high concentrations. The data were fully consistent with a mechanism in which the Ru metal center in the excited state accepts an electron from iodide to form an iodine atom and, within 70 ns, that atom reacts with the iodide associated with the ligand to yield $I_2^{\bullet-}$. This rapid formation of an I−I bond was facilitated by the supramolecular assembly of the three reactant ions necessary for this ter-ionic reaction that is relevant to solar fuel production.

Supramolecular chemistry, where chemical species are held together through non-covalent interactions, has impacted the fields of host−guest chemistry,[1−3] chromatography,[4] catalysis[5,6] and artificial photosynthesis.[7] In natural and artificial photosynthesis, light absorption and catalysis are separate processes,[8−17] yet integration into one could potentially be more efficient and require fewer materials. In a move toward this goal a tetra-cationic ruthenium polypyridyl chromophore, $[Ru(dtb)_2(tmam)]^{4+}$ (here **Ru^{4+}**), where dtb is 4,4′-di-*tert*-butyl-2,2′-bipyridine and tmam is 4,4′-bis-(trimethylaminomethyl)-2,2′-bipyridine (Figure 1), was ion-paired with iodide ions in acetone solution. ^{1}H NMR, UV−vis and density functional theory (DFT) studies revealed that two iodides were ion-paired, one associated with the tmam ligand and the second was closer to the Ru metal center. Classical Stern−Volmer analysis revealed upward curvature with saturation at high iodide concentrations, behavior consistent with a mechanism where electron transfer forms an iodine atom that reacts with iodide to yield a covalent I−I bond within the ter-ionic complex.[18,19] Hence, supramolecular chemistry allows two reactants to be brought into contact with a visible light absorbing chromophore that upon light excitation yields chemical bonds of relevance to solar energy conversion.

The **Ru^{4+}** complex was designed to include two important structural features: (1) a dicationic tmam ligand that has previously been shown to possess an iodide binding pocket;[20,21] and (2) two ancillary dtb ligands that encouraged the iodide ions to ion-pair proximate to the tmam pocket. The excited-state reduction potential was also tuned with the electron donating alkyl substituents in the 4 and 4′ position of 2,2′-bipyridine that decreased the oxidizing strength of the excited state.

Iodide titration into an acetone solution of **Ru^{4+}** with an ^{1}H NMR assay provided atomistic information on the ion-pair structure. Iodide additions induced dramatic upfield shifts of the 3 and 3′ H atom resonances associated with the tmam ligand, which were the most acidic in the complex, with no significant change to the 3,3′-H resonances of the dtb ligands, Figure 1d. The roofed-doublet pattern for the methylene H atoms has been previously reported and is fully consistent with the presence of an iodide in the tmam pocket, Figure 1e.[20,21] A second site for iodide interaction was identified through a large upfield shift of the 5 and 6 H atoms of the dtb ligand consistent with association of a second iodide near the Ru center. DFT calculations predicted a very similar optimized structure with one iodide in the tmam pocket and the other about 5.8 Å away, between the diimine ligands and more proximate to the Ru metal center, Figure 1e.

The visible absorption spectrum of **Ru^{4+}** displayed a metal-to-ligand charge transfer (MLCT) absorption band near 450 nm (Figure 1a).[22] The addition of iodide resulted in a small blue shift of this band and a substantial increase in the absorbance at 330 nm. Titration data were best described with two equilibrium constants $K_{eq\ 1} = 1.7 \pm 0.5 \times 10^6\ M^{-1}$ and $K_{eq\ 2} = 1.5 \pm 0.5 \times 10^5\ M^{-1}$ corresponding to the singly and doubly iodide paired species, respectively. Importantly, the 10-fold difference in equilibrium constants had implications for the excited-state reactivity described below. For example, almost equal concentrations of the two ion-paired species were present with 3 equiv of iodide, while nearly complete conversion to the more interesting doubly ion paired species required greater than 10 equiv of iodide (Figure S4).

Light excitation into the MLCT band resulted in room temperature photoluminescence (PL) with a maximum at 685 nm. The PL spectrum measured at 77K was modeled with a

Received: May 11, 2018
Published: June 13, 2018

Downloaded via UNIV OF NORTH CAROLINA on November 8, 2020 at 18:56:33 (UTC).
See https://pubs.acs.org/sharingguidelines for options on how to legitimately share published articles.

© 2018 American Chemical Society

DOI: 10.1021/jacs.8b04961
J. Am. Chem. Soc. 2018, 140, 7799−7802

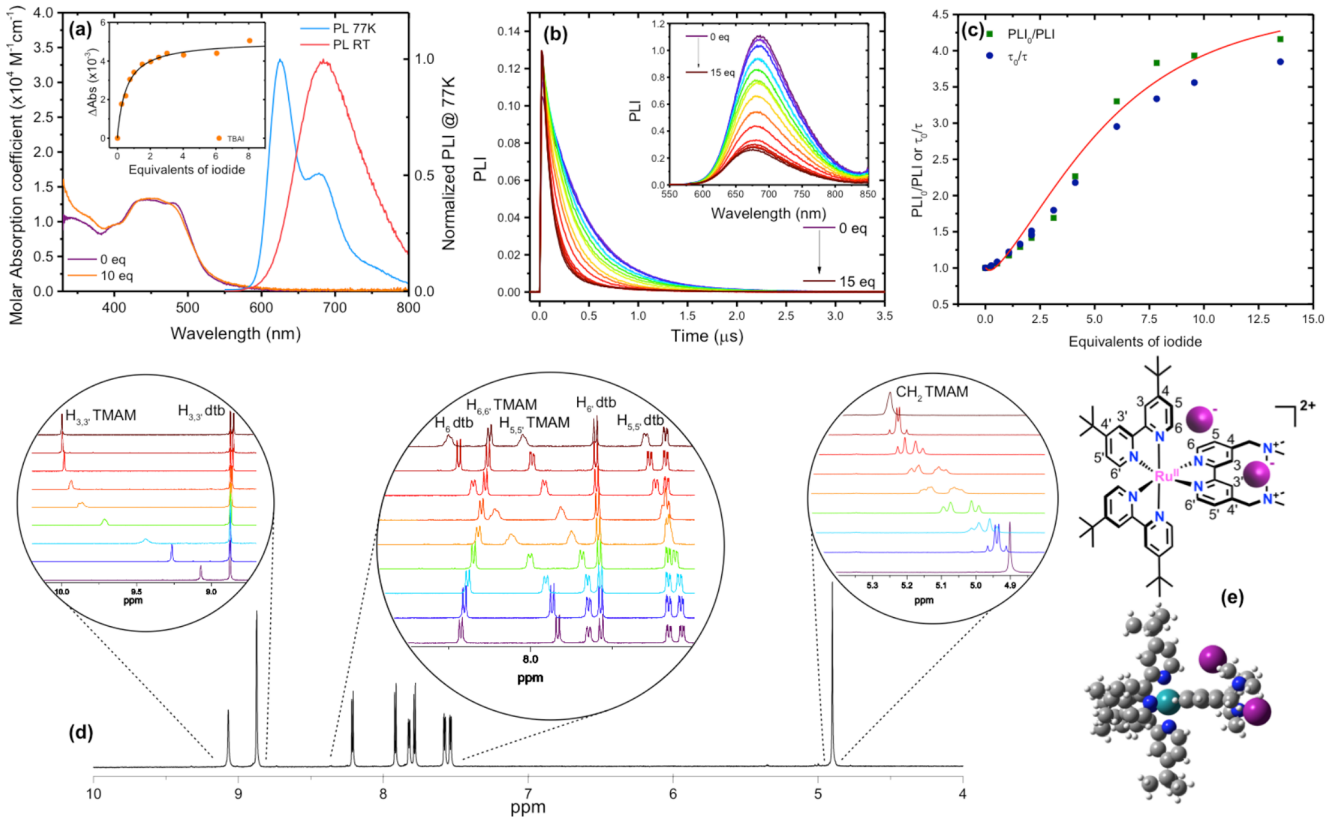

Figure 1. (a) UV−vis absorption spectrum of $\mathbf{Ru}^{4+}$ upon titration of TBAI in acetone. The inset shows the change in ground state absorption at 460 nm for $\mathbf{Ru}^{4+}$ upon titration of TBAI. The photoluminescence (PL) spectra of $\mathbf{Ru}^{4+}$ in acetone at room temperature (red) and in butyronitrile at 77 K (blue) are also shown. (b) Time-resolved PL decays of $\mathbf{Ru}^{4+}$* (10 μM) with the addition of up to 15 equiv of TBAI. Inset shows the corresponding steady-state PL spectra with the addition of up to 15 equiv of TBAI. (c) Stern−Volmer analysis of the data in panel b with fit overlaid according to a modified Stern−Volmer equation. (d) ^{1}H NMR spectra of $\mathbf{Ru}^{4+}$ in deuterated acetone (black). Each circle represents the chemical shifts observed upon titration of TBAI between 0 equiv (bottom) and 5 equiv (top) in deuterated acetone. (e) $\mathbf{Ru}^{4+}$ ion-paired with two iodides in positions consistent with ^{1}H NMR spectral shifts. 3D rendering of the DFT optimized structure has been added to guide the eye.

Franck−Condon line-shape analysis[23,24] that provided an estimate of the Gibbs free energy stored in the excited state ΔG_{ES} = 1.98 V. With this value and the first reduction potential of the complex at −0.77 V vs NHE, the excited-state reduction potential was estimated to be ($E°(\mathbf{Ru}^{4+*/3+})$ = 1.21 V vs NHE), which is within 20 mV of the accepted reduction potential of iodide $E°(I^{-/\bullet})$ = 1.23 V vs NHE.[25]

Novel excited-state quenching behavior was observed in iodide titration experiments. The PL spectra were found to slightly blue-shift by 15 nm, which corresponded to 30 meV. Furthermore, the PL spectra decreased in intensity when up to 10 equiv of iodide were added, after which the spectra were largely insensitive to additional iodide, Figure 1b. Time resolved PL decays measured after pulsed light excitation were exponential, τ_o= 450 ns, and the lifetimes decreased with added iodide and again saturated at 120 ns when >10 equiv were present. Interestingly, no excited-state quenching was observed in 50 mM tetrabutylammonium perchlorate ($TBAClO_4$) acetone solutions corroborating the importance of the supramolecular iodide ion-paired complex.

Stern−Volmer plots of the quenching data are shown in Figure 1c that reveal upward curvature followed by saturation at high iodide concentrations. Such upward curvature is often invoked when both static and dynamic (diffusional) quenching are operative. In the classic model, the "static" component corresponds to a ground state adduct that is completely nonluminescent.[26,27] In contrast, the adduct formed here is luminescent with a lifetime of 120 ns. The overlaid red curve was based on the presence of three photoluminescent species that are as follows: (i) the initial complex with an excited-state lifetime τ_0 = 450 ns, (ii) a singly ion-paired species with the same lifetime that was dynamically quenched by iodide, and (iii) the ter-ionic species with an excited-state lifetime of 120 ns.

Nanosecond transient absorption spectroscopy was used to unravel the excited-state reaction chemistry. Figure 2c shows transient difference spectra measured after pulsed light excitation of $\mathbf{Ru}^{4+}$ in the presence of excess iodide. Overlaid is a simulation based on the formation of a 1:1 mixture of the reduced Ru complex, $\mathbf{Ru}^{3+}$, and $I_2^{\bullet-}$.

The $\mathbf{Ru}^{4+}$* excited-state spectra revealed two isosbestic points that were conveniently located near the absorption maxima of the two reaction products: 400 nm ($I_2^{\bullet-}$) and 541 nm ($\mathbf{Ru}^{3+}$). Kinetic data at these isosbestic points as a function of the iodide concentration are shown in Figure 2a,b. Upon initial addition of iodide, the rates increased with the I^- concentration from which rate constants for the formation of $\mathbf{Ru}^{3+}$ (k_{Ru} = 2.5 ± 0.3 × 10^{10} M^{-1} s^{-1}) and for $I_2^{\bullet-}$ (k_I = 1.7 ± 0.1 × 10^{10} M^{-1} s^{-1}) were obtained. However, when greater than 10 equiv of I^- were present, the rates became I^- independent with $k_{obs}(\mathbf{Ru}^{3+})$ = 1.3 ± 0.1 × 10^7 s^{-1} and $k_{obs}(I_2^{\bullet-})$ = 1.2 ± 0.1 × 10^7 s^{-1}. The insensitivity to the I^- concentration was consistent with the electron transfer reactivity occurring within the ion-pair. The rate constant for

DOI: 10.1021/jacs.8b04961
J. Am. Chem. Soc. 2018, 140, 7799−7802

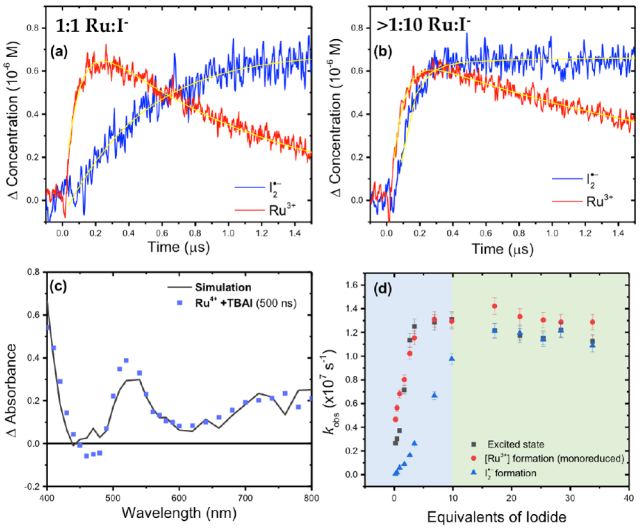

Figure 2. Single wavelength absorption changes measured after pulsed light excitation of $\mathbf{Ru}^{4+}$ with 1 equiv (a) and 25 equiv (b) of TBAI in acetone with an overlaid fit in yellow. (c) Transient absorption difference spectra obtained 500 ns after pulsed light excitation of a solution containing $\mathbf{Ru}^{4+}$ and TBAI. Overlaid is a simulation based on the formation of a 1:1 mixture of the reduced Ru complex, $\mathbf{Ru}^{3+}$, and $I_2^{\bullet-}$. (d) Observed rate constants for the formation of the $\mathbf{Ru}^{3+}$ complex and $I_2^{\bullet-}$ as a function of the iodide equivalents. The region highlighted in blue corresponds to dynamic quenching whereas that in green corresponds predominantly to the static bond formation within the ion pair.

the formation of $I_2^{\bullet-}$ was determined to be $3.1 \pm 0.3 \times 10^{10}$ M^{-1} s^{-1} (Figure S5). In the saturation region, the formation of $I_2^{\bullet-}$ was substantially slower (by a factor of 5 at 1.7 mM I^-) than what would be expected for diffusional $I_2^{\bullet-}$ formation.

The kinetic data demonstrate that $\mathbf{Ru}^{3+}$ was a primary photoproduct, which appeared with the same rate constant as excited-state decay, while $I_2^{\bullet-}$ appeared on a longer time scale that was attributed to the reaction of the iodine atom with iodide in the ion-pair at high iodide concentrations. The ter-ionic complex formed enables a more detailed description of the light induced bond formation that is discussed below with the help of Scheme 1.

The ground-state structure locates one iodide in the tmam pocket and another iodide between the ligands and more proximate to the Ru^{II}. DFT calculations indicate the two iodides are about 5.8 Å apart. Light excitation formally oxidizes the metal center and reduces the tmam ligand and the resultant excited-state dipole influences the ter-ionic structure. Coulombic repulsion will move the iodide in the tmam pocket away from the 3,3′-H atoms of the bipyridine toward the cationic amines. Indeed, prior research has shown full photorelease of chloride anions associated with a ligand where the excited state resides.[28] Coulombic repulsion of the other iodide is expected to be less, as it is not directly associated with the tmam ligand, and may be attracted to the more Lewis acidic Ru^{III}.

This iodide is hence more strongly coupled to the Ru in the excited state and is the one that likely transfers an electron to the metal center. Further evidence for this elementary reaction comes from the observation that static excited-state quenching was absent within the first tmam ion-paired species. Furthermore, DFT calculations[29] estimated a stabilization of nearly 48 kJ/mol upon ion-pairing (Figure S6), which is close

Scheme 1. Proposed Mechanism for Visible Light Excitation of $\{Ru^{4+},2I^-\}$ To Yield an I–I Bond within the Supramolecular Complex

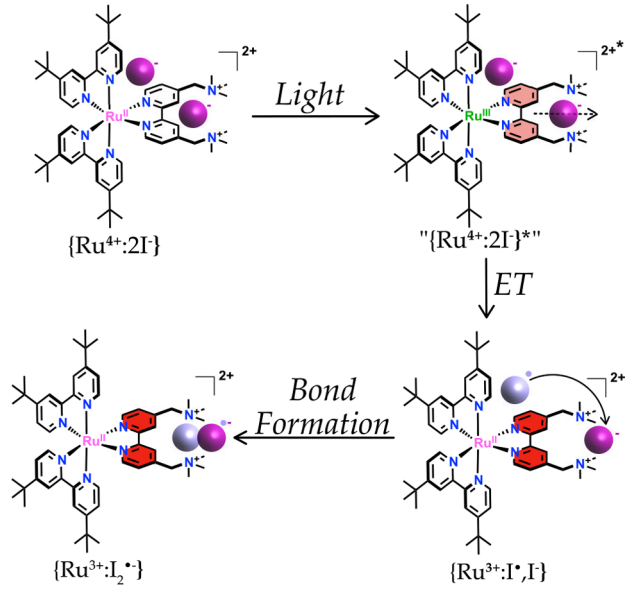

to the 35 kJ/mol obtained from the equilibrium constant. Hence, the data support a mechanism where the tmam ion-paired iodide was stabilized to such an extent that the excited state did not oxidize it.

Electron transfer from the proximate iodide forms the reduced Ru^{II} complex that will have even greater electron density on the tmam ligand and hence stronger repulsion toward the iodide in the pocket. The iodine atom, on the other hand, will be polarized by this field but as a neutral atom will not experience the Coulombic repulsion of the iodide ion. Within 60 ns, the iodine atom then moves a few angstroms to react with the iodide ion to form $I_2^{\bullet-}$ with an I–I bond distance of 3.1 Å.[30] This mechanism points toward the importance of the excited state being localized on the ligand that initially ion-pairs with iodide and suggests that more rapid bond formation will be realized with excited state localized away from the reaction site.

In conclusion, a ter-ionic complex was prepared through the rational design of a Ru complex bearing a dicationic tmam ligand with an iodide binding pocket as well as steric constraints that keep the second iodide in close proximity. Upon visible light excitation, this ter-ionic excited-state complex underwent "intra-ionic" electron transfer and successive covalent I–I bond formation that gave rise to novel excited-state quenching. More generally, supramolecular assembly with ions provides the opportunity to spatially arrange reactants at desired locations prior to light excitation that are necessarily maintained in the initially formed excited-state. Hence, utilizing excited-states to make covalent bonds within ter-ionic complexes precludes the need for diffusion and may ultimately enhance specificity for more widespread applications in photocatalysis.

■ ASSOCIATED CONTENT

Supporting Information

The Supporting Information is available free of charge on the ACS Publications website at DOI: 10.1021/jacs.8b04961.

DOI: 10.1021/jacs.8b04961
J. Am. Chem. Soc. 2018, 140, 7799–7802

Experimental details, characterization for newly reported compound (PDF)

AUTHOR INFORMATION

Corresponding Author

*gjmeyer@email.unc.edu

ORCID

Ludovic Troian-Gautier: 0000-0002-7690-1361
Renato N. Sampaio: 0000-0002-7158-6470
Lionel Marcélis: 0000-0002-6324-477X
Gerald J. Meyer: 0000-0002-4227-6393

Author Contributions

§These authors contributed equally.

Notes

The authors declare no competing financial interest.

ACKNOWLEDGMENTS

The University of North Carolina (UNC) authors acknowledge support from the Division of Chemical Sciences, Office of Basic Energy Sciences, Office of Energy Research, U.S. Department of Energy (Grant DE-SC0013461). L.T.-G. acknowledges the Belgian American Educational Foundation (BAEF) as well as the Bourse d'Excellence Wallonie-Bruxelles International (WBI.World) for postdoctoral funding. The authors acknowledge Wesley Swords for the gift of tmam ligand as well as the University of North Carolina's Department of Chemistry Mass Spectrometry Core Laboratory.

REFERENCES

(1) De Leener, G.; Moerkerke, S.; Lavendomme, R.; Reinaud, O.; Jabin, I. Calix[6]azacryptand-Based Receptors. In *Calixarenes and Beyond*; Neri, P., Sessler, J., Wang, M. X., Eds.; Springer: Cham, 2016.
(2) Lehn, J.-M. *Angew. Chem., Int. Ed. Engl.* **1988**, *27*, 89−112.
(3) Armaroli, N.; Chambron, J.-C.; Collin, J.-P.; Dietrich-Buchecker, C.; Flamigni, L.; Kern, J.-M.; Sauvage, J.-P. Metal-Assembled Catenanes, Rotaxanes, and Knots. In *Electron Transfer in Chemistry*; Balzani, V., Ed.; Wiley-VCH Verlag GmbH: Weinheim, Germany, 2001.
(4) Hancock, W. S.; Bishop, C. A.; Prestidge, R. L.; Harding, D. R.; Hearn, M. T. *Science* **1978**, *200*, 1168−1170.
(5) Brak, K.; Jacobsen, E. N. *Angew. Chem., Int. Ed.* **2013**, *52*, 534−561.
(6) Parmar, D.; Sugiono, E.; Raja, S.; Rueping, M. *Chem. Rev.* **2014**, *114*, 9047−9153.
(7) Casarin, L.; Swords, W.; Caramori, S.; Bignozzi, C. A.; Meyer, G. J. *Inorg. Chem.* **2017**, *56*, 7324−7327.
(8) Barber, J. *Chem. Soc. Rev.* **2009**, *38*, 185−196.
(9) McEvoy, J. P.; Brudvig, G. W. *Chem. Rev.* **2006**, *106*, 4455−4483.
(10) Fukuzumi, S.; Ohkubo, K.; Suenobu, T. *Acc. Chem. Res.* **2014**, *47*, 1455−1464.
(11) Hwang, S. J.; Powers, D. C.; Maher, A. G.; Anderson, B. L.; Hadt, R. G.; Zheng, S.-L.; Chen, Y.-S.; Nocera, D. G. *J. Am. Chem. Soc.* **2015**, *137*, 6472−6475.
(12) Kainz, Q. M.; Matier, C. D.; Bartoszewicz, A.; Zultanski, S. L.; Peters, J. C.; Fu, G. C. *Science* **2016**, *351*, 681−684.
(13) Welin, E. R.; Le, C.; Arias-Rotondo, D. M.; McCusker, J. K.; MacMillan, D. W. C. *Science* **2017**, *355*, 380−385.
(14) Michelet, B.; Deldaele, C.; Kajouj, S.; Moucheron, C.; Evano, G. *Org. Lett.* **2017**, *19*, 3576−3579.
(15) Huynh, M. H. V.; Meyer, T. J. *Chem. Rev.* **2007**, *107*, 5004−5064.
(16) Romero, N. A.; Nicewicz, D. A. *Chem. Rev.* **2016**, *116*, 10075−10166.
(17) Hu, K.; Sampaio, R. N.; Marquard, S. L.; Brennaman, M. K.; Tamaki, Y.; Meyer, T. J.; Meyer, G. J. *Inorg. Chem.* **2018**, *57*, 486−494.
(18) Nord, G. *Comments Inorg. Chem.* **1992**, *13*, 221−239.
(19) Stanbury, D. M.; Wilmarth, W. K.; Khalaf, S.; Po, H. N.; Byrd, J. E. *Inorg. Chem.* **1980**, *19*, 2715−2722.
(20) Swords, W. B.; Li, G.; Meyer, G. J. *Inorg. Chem.* **2015**, *54*, 4512−4519.
(21) Wehlin, S. A. M.; Troian-Gautier, L.; Li, G.; Meyer, G. J. *J. Am. Chem. Soc.* **2017**, *139*, 12903−12906.
(22) Troian-Gautier, L.; Moucheron, C. *Molecules* **2014**, *19*, 5028−5087.
(23) Chen, P.; Meyer, T. J. *Chem. Rev.* **1998**, *98*, 1439−1478.
(24) Damrauer, N. H.; Boussie, T. R.; Devenney, M.; McCusker, J. K. *J. Am. Chem. Soc.* **1997**, *119*, 8253−8268.
(25) Wang, X.; Stanbury, D. M. *Inorg. Chem.* **2006**, *45*, 3415−3423.
(26) Lakowicz, J. R. *Principles of Fluorescence Spectroscopy*; Plenum Press: New York, 1983.
(27) Valeur, B.; Berberan-Santos, M. N. *Molecular Fluorescence*; Wiley-VCH: Weinheim, Germany,2012; pp 141−179.
(28) Turlington, T. D.; Troian-Gautier, L.; Sampaio, R. N.; Beauvilliers, E. E.; Meyer, G. J. *Inorg. Chem.* **2018**, *57*, 5624−5631.
(29) Troian-Gautier, L.; Beauvilliers, E. E.; Swords, W. B.; Meyer, G. J. *J. Am. Chem. Soc.* **2016**, *138*, 16815−16826.
(30) Chanon, M.; Rajzmann, M.; Chanon, F. *Tetrahedron* **1990**, *46*, 6193−6299.

DOI: 10.1021/jacs.8b04961
J. Am. Chem. Soc. 2018, 140, 7799−7802